

High-Temperature Pyrolysis for Elimination of Per- and Polyfluoroalkyl Substances (PFAS) from Biosolids

Authors:

Hanieh Bamdad, Sadegh Papari, Emma Moreside, Franco Berruti

Date Submitted: 2023-02-20

Keywords: PFAS, biosolids, high-temperature pyrolysis, thermal treatment, biochar

Abstract:

Biosolids generated as byproducts of wastewater treatment processes are widely used as fertilizer supplements to improve soil condition and ultimately agricultural products yields and quality. However, biosolids may contain toxic compounds, i.e., per- and polyfluoroalkyl substances (PFAS), which can end up in soils, groundwater, and surface water, causing adverse environmental and health effects. The purpose of this study was to investigate the application of High-Temperature Pyrolysis (HTP) treatment for biosolids management, and its efficacy in eliminating PFAS from the solid fraction. Biosolid samples were pyrolyzed at two different temperatures, 500 and 700 °C, in a continuous bench-scale pyrolysis unit. The major finding is that the treatment process at higher pyrolysis temperatures can remarkably reduce or eliminate the level of PFAS (by ~97?100 wt%) in the resulting biochar samples.

Record Type: Published Article

Submitted To: LAPSE (Living Archive for Process Systems Engineering)

Citation (overall record, always the latest version):

LAPSE:2023.0706

Citation (this specific file, latest version):

LAPSE:2023.0706-1

Citation (this specific file, this version):

LAPSE:2023.0706-1v1

DOI of Published Version: <https://doi.org/10.3390/pr10112187>

License: Creative Commons Attribution 4.0 International (CC BY 4.0)

Article

High-Temperature Pyrolysis for Elimination of Per- and Polyfluoroalkyl Substances (PFAS) from Biosolids

Hanieh Bamdad ¹, Sadegh Papari ^{1,*}, Emma Moreside ² and Franco Berruti ^{1,*}

¹ Institute for Chemicals and Fuels from Alternative Resources (ICFAR), Department of Chemical and Biochemical Engineering, Western University, London, ON N0M 2A0, Canada

² Char Technologies Ltd., 403-789 Don Mills Rd., Toronto, ON M3C 1T5, Canada

* Correspondence: spapari@uwo.ca (S.P.); fberruti@uwo.ca (F.B.)

Abstract: Biosolids generated as byproducts of wastewater treatment processes are widely used as fertilizer supplements to improve soil condition and ultimately agricultural products yields and quality. However, biosolids may contain toxic compounds, i.e., per- and polyfluoroalkyl substances (PFAS), which can end up in soils, groundwater, and surface water, causing adverse environmental and health effects. The purpose of this study was to investigate the application of High-Temperature Pyrolysis (HTP) treatment for biosolids management, and its efficacy in eliminating PFAS from the solid fraction. Biosolid samples were pyrolyzed at two different temperatures, 500 and 700 °C, in a continuous bench-scale pyrolysis unit. The major finding is that the treatment process at higher pyrolysis temperatures can remarkably reduce or eliminate the level of PFAS (by ~97–100 wt%) in the resulting biochar samples.

Keywords: PFAS; biosolids; high-temperature pyrolysis; thermal treatment; biochar



Citation: Bamdad, H.; Papari, S.; Moreside, E.; Berruti, F.

High-Temperature Pyrolysis for Elimination of Per- and Polyfluoroalkyl Substances (PFAS) from Biosolids. *Processes* **2022**, *10*, 2187. <https://doi.org/10.3390/pr10112187>

Academic Editor: Bipro R. Dhar

Received: 26 September 2022

Accepted: 20 October 2022

Published: 25 October 2022

Publisher's Note: MDPI stays neutral with regard to jurisdictional claims in published maps and institutional affiliations.



Copyright: © 2022 by the authors. Licensee MDPI, Basel, Switzerland. This article is an open access article distributed under the terms and conditions of the Creative Commons Attribution (CC BY) license (<https://creativecommons.org/licenses/by/4.0/>).

1. Introduction

In water resource recovery facilities (WRRF), solid wastewater byproducts, known as biosolids, are separated through several consecutive treatment steps [1]. Biosolids are rich in micronutrients and, when used as fertilizer supplements, offer many beneficial effects to soil properties, such as improving plant growth, cation exchange capacity, porosity, bulk density, and water holding capacity [2]. In some countries, land application of biosolids is more prevalent than in others, compared to incineration and landfill, due to higher disposal cost [3]. According to the literature, 660,000 dry tonnes of biosolids are produced annually in Canada, 43% of which are utilized for land applications [4]. In the United States, approximately 55% of seven million dry tonnes of biosolids, generated from WRRF, were applied to soil in 2004 [5]. In Australia, 75% of all biosolids produced are currently diverted to land application for soil amendment [6].

In contrast to the beneficial effects, the potential presence of contaminants in biosolids, e.g., per- and polyfluoroalkyl substances (PFAS) [7,8] has gained attention due to the serious human-health issues that have been identified, including certain types of cancer, liver damage, cardiovascular problems, birth defects, and immune system disorders [9]. PFAS are a series of anthropogenic chemicals that have been traditionally used in fabrics and industrial materials with nonstick and oil/water repellent properties, such as carpets, food packaging, Teflon coatings, and fire-fighting foams [10]. Given that PFAS molecules are structures with short and strong C-F chemical bonds with functional groups containing oxygen (O), hydrogen (H), nitrogen (N), and sulfur (S), they are extremely stable and, as such, they have been called 'forever chemicals'. There are nearly 8000 types of PFAS compounds, including short ($\leq C7$ for PFCAs and $\leq C5$ for PFSAs) and long-chain ($\geq C8$ for PFCAs and $\geq C6$ for PFSAs), the most commonly used since 1940s being perfluorooctanoic acid (PFOA) and perfluorooctanesulfonic acid (PFOS) [11]. In consideration of toxicity, recalcitrance, and persistency of PFAS compounds, the United States Environmental Protection Agency

(US EPA) decided to phase out both PFOA and PFOS in 2000 and mandate the complete elimination of PFOA in 2016 [12]. Further, in 2009, the US EPA set a lifetime health advisory level (HAL) to an individual maximum of 70 ng/L (ppt) in drinking water for both PFOA and PFOS, excluding other PFAS types [13]. Likewise, the European Union (EU) targeted a limit value of 100 ng/L in 2019 for the sum of 12 PFAS in drinking water [14].

Several treatment technologies have been under investigation to capture and destroy effluents containing PFAS. Degradation methods by chemical agents are associated with providing energy for strong C-F bond dissociation [15]. Photocatalysis using UV sources [16], electrocatalysis as a fast oxidation process [17], oxidation–reduction reactions under aqueous conditions [18,19], and sonochemical degradation via ultrasonic field [20] have been identified as the most promising chemical approaches for the removal of PFAS. Most biological efforts using microbes or enzymes for PFAS destruction have not shown much promise due to in situ limitations, low efficiency, long degradation times, and complexity in both laboratory-scale and field applications [21]. Reverse osmosis, ion-exchange resins, and granular activated carbon [22] have been shown as able to trap/physically absorb/adsorb the PFAS molecules. However, the efficiency of these methods quickly degrades due to fouling, and the PFAS persist in the resulting concentrated waste streams [23].

Thermal treatment technologies can use high temperatures to destroy the PFAS chemical structures by breaking the C-C and C-F bonds. Thermal processing, such as combustion, pyrolysis, gasification, and hydrothermal liquefaction, are considered as emerging technologies under development and, consequently little is known about their PFAS destruction performance during biosolid waste treatment [24,25]. Incineration usually occurs at temperatures ranging between 1600 and 2000 °C to eliminate the PFOA and PFOS adsorbed by granular activated carbon (GAC) [26]. The side effect of this method is the formation of harmful emissions with long lifetime effects, such as dioxins and furans [27]. Moreover, GAC does not perform well in the adsorption of short-chain PFAS family compounds [28].

Pyrolysis is a thermochemical conversion method of upgrading biomass ‘wastes’ (including PFAS-containing biosolids and sewage sludge) into valuable solid and gaseous products, commonly called biochar and pyrogas, by heating the feedstock to intermediate or high temperatures (between 500 and 850 °C) in the absence of oxygen.

The current scientific articles on the fate of PFAS by thermal processes are very limited. This work aims to examine the application of pyrolysis for the removal of PFAS contaminants from biosolids focusing on advantages of (I) producing value-added outputs, (II) determining the end-of-life of PFAS in the environment, (III) reducing organic waste mass, and (IV) concurrently generating pyrolysis gas as an energy/alternative fuel.

2. Materials and Methods

2.1. Biosolids

Dried biosolids were derived from unstabilized waste activated sludge produced from three water resource recovery sites from across the USA (referred to as S1, S2, and S3). The solids were previously dewatered with belt filter presses to approximately 20 wt% solids and subsequently dried in a batch thermal dryer fired with natural gas to evaporate water, resulting in a biosolids product that included approximately 93 wt% solids.

2.2. Pyrolysis Reactor

The bench-scale Mechanically Fluidized Reactor (MFR) (pyrolyzer), seen in Figure 1, is composed of two main sections: the reactor and the condensation system. The reaction section includes a mechanically fluidized cylindrical vessel, 15 cm in diameter and 25 cm in height. An induction unit is used to provide the heat. Five hundred grams of feedstock are precisely weighed and then introduced into the hopper. A screw feeder conveys the feedstock from the hopper to the reactor at a rate of 25 g/min. The feedstock is well mixed inside the reactor operating at either 500 or 700 °C via a mechanical agitator driven by an electrical motor. The condenser apparatus is composed of two condensers in series placed in a cold-water bath, where a mixture of ice and water is used for cooling. After the second

condenser, the residual gas goes through a cotton filter and then to the exhaust line where it can be sampled and characterized. A screw connected to the bottom of the reactor is used to extract the biochar, which is then collected in a sealed biochar container.

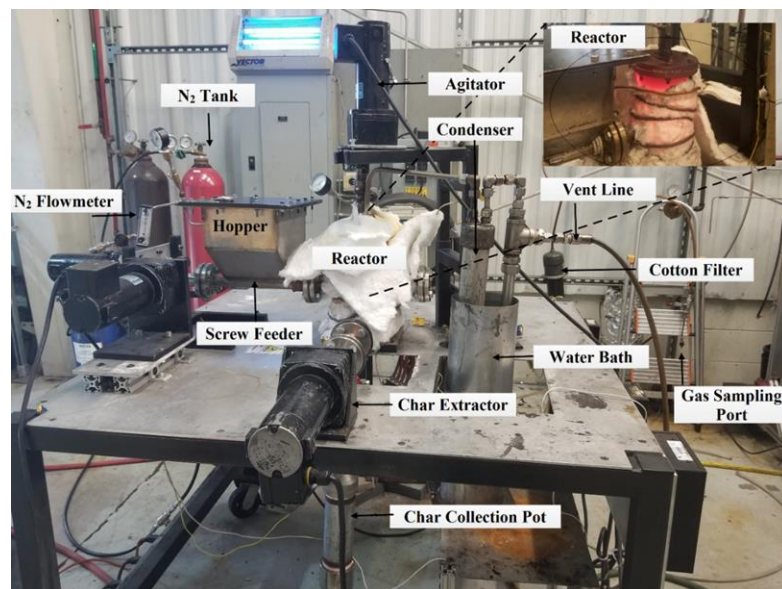


Figure 1. Bench-scale MFR and the main reactor (top-right corner).

2.3. Biosolid and Biochar Sampling and Analysis

ICFAR, along with the third-party analytical laboratories including ORTECH (located in Mississauga, ON, Canada), ALS (London, ON, Canada), and E3 Laboratories (Niagara-on-the-Lake, ON, Canada), analyzed the feedstock biosolids and the biochar/bio-oil/pyrogas outputs for PFAS, and performed proximate and ultimate analysis, ash characterization, and calorific value analysis on both the biosolids and the biochar outputs.

2.3.1. Ultimate Analyses

Elemental analysis of carbon, hydrogen, nitrogen, and sulfur was performed using the CHNS elemental analyzer, 'Thermo Flash EA 1112'. Samples were combusted at 900 °C in a stream of helium with a measured amount of oxygen. The produced N₂, CO₂, H₂O, and SO₂ were then separated and quantified by gas chromatography using a 5 mm diameter steel packed column 2 m long, a helium carrier gas with a flow rate of 140 mL/min, and detected with a thermal conductivity detector (TCD). The oxygen content was calculated by the mass difference. BBOT (2,5-Bis (5-tert-butyl-benzoxazol-2-yl) thiophene), 1–2 mg, was used as a standard to calibrate the system.

2.3.2. Calorific Value

A bomb calorimeter (C200, IKA, Wilmington, NC, USA) was used to measure the higher heating values with two replicates per sample, based on the D4809-00 ASTM method. The calibration process was performed in the sample vessel using pelletized benzoic acid (IKA C 723, IKA, Germany) with a combustion heat of 26.45 MJ/kg.

2.3.3. Ash Characterization

Ash characterization was undertaken by E3 Labs for the analysis of metals by Inductively Coupled Plasma Optical Emission Spectrometry (ICP-OES). This method includes a very strong acid digestion procedure that dissolves most elements that could become 'environmentally available' in biosolid samples.

2.3.4. Proximate Analysis

The ASTM standard D1762-84 was selected to determine moisture, volatile matter, and ash in the biosolid samples. Specifically, moisture was determined as loss in weight in a muffle furnace at 105 °C for 2 h. Volatile matter was characterized as loss in weight at 950 °C for 6 min. Ash content was calculated as the residue after burning to constant weight at 750 °C for 6 h.

2.3.5. Material Balance

Five hundred grams of biomass were precisely weighed and, after each test, biooil and biochar were collected and weighed by a balance with 0.1 g accuracy. The pyrogas yield was calculated by the weight difference. The yields were calculated on a dry biosolid mass basis:

$$\text{Biooil yield} = (\text{g biooil/g biosolid}) \times 100$$

$$\text{Biochar yield} = (\text{g biochar/g biosolid}) \times 100$$

$$\text{Noncondensable pyrogas yield} = 100 - \text{biooil yield} - \text{biochar yield}$$

2.4. Gas Sampling and PFAS Analysis

Sampling for PFAS was conducted using the sampling procedures detailed in 'Modified Method for Determining hexafluoropropylene oxide dimer acid (HFPO-DA) and Other Method 537 PFAS Compound Emissions in Stack Gas'. Currently, there are no standardized and mandated emission testing and analysis methods for PFAS, although the US EPA is in the process of developing such methods. The sampling approach used by ORTECH was based on discussions and feedback from technical contacts at ALS Environmental (ALS), the laboratory which prepared the sampling media and conducted the analysis of the samples collected by ORTECH. Briefly, the sampling method involved withdrawing a sample of the stack gas (~3 L per minute) through a sampling line containing a glass wool plug to remove particulate material. The sample was then passed through a water-cooled condenser and a XAD-2 adsorbent tube, as the primary collection device. Condensate was collected in a series of impingers initially containing DI water and the sample was then drawn through a backup XAD-2 adsorbent tube. The sampled gas stream then passed through a silica gel trap to remove any remaining traces of moisture prior to the rotameter, pump, and dry gas meter. ORTECH started and stopped each test as instructed by the operator.

Following the conclusion of each run, the tubes were removed from the train, capped, and placed in appropriately labeled test tubes which were also capped. The probe and condenser were rinsed in triplicate with a methanol/5% (*v/v*) NH₄OH solution into a sample container. The impinger solution and collected condensate was then transferred into a separate sample container. The samples were sealed and sent to ALS for PFAS analysis.

The ALS analytical laboratory analyzed three separate sample fractions (probe/condenser rinse, XAD-2 tube, and impinger solution) specifically for thirty-one individually measured gas-phase PFAS compounds. A blank of each sample fraction was also collected and analyzed to assess background contamination, if any. The amounts collected in each fraction were combined to determine the total collected for each sample. The analytical detection limit was used to determine the total collected and emission data, for those compounds reported as less than the analytical detection limit (<). The detection limit for each of the PFAS compounds was different.

2.5. Pyrolysis Gas Characterization

To calculate the concentration of the various PFAS components in the pyrogas, the summation of three sample sources (probe/condenser, XAD-2, and impinger solution) was utilized. A value of zero was assumed for concentrations below detection limits. The total volume of gas sampled, corrected to 1 atm and 25 °C, was provided by ORTECH. Therefore,

the total mass of gas sampled was calculated by determining the number of moles using the ideal gas law multiplied by the molecular density of air (29 g/mol).

$$n = (P \times V)/(R \times T)$$

where n is the number of moles, P is the pressure, V is the gas volume, R is the ideal gas constant (8.314 Pa.m³/K.mol), and T is the standard temperature of 298 K.

The total mass of each PFAS component was then divided by the mass of gas in each sample to determine the concentration (w/w).

3. Results

To prevent bioaccumulation of toxic PFAS in organisms from biosolids through different exposure routes, such as soil and groundwater, the biosolids must be treated competently. According to the literature, under the high-temperature and oxygen-free conditions of the typical pyrolysis reactions, the PFAS compounds are volatilized out of the solids, and then destroyed through a hydrodefluorination (HDF) pathway in which the carbon–fluorine (C-F) bond is converted into a carbon–hydrogen (C-H) bond, where the hydrogen is supplied from the steam-reforming reaction [24]. Steam-reforming is a method for generating hydrogen by reaction of primary pyrolysis products (hydrocarbons) with the moisture of the feedstock.

3.1. PFAS Analytical Results

The bench-scale HTP system, which operates as a continuously mixed bed reactor, processed biosolids (named herein as S1–S3) under pyrolysis temperatures of 500 and 700 °C. A summary of the results for PFAS in solids (biosolids, biochar at 500 °C, and biochar at 700 °C), biooil, and pyrolysis gas (pyrogas) is presented in Table 1. For clarity, the PFAS components that are measurable in any of the phases or samples tested are bolded, while the full suite of samples tested is presented. Of the twenty-nine PFAS compounds included in the test program, only nine were detected in quantities greater than the analytical detection limit in at least one of the biosolid samples.

The average concentration of PFAS compounds was 36.7 ppb or µg/kg of biosolids, considering the major contribution of Perfluorooctane sulfonic acid (PFOS) in the total detected PFAS. There are currently no US EPA regulations for managing PFAS in biosolids, yet the PFAS content in all three biosolid samples is higher than a maximum lifetime health advisory level (HAL) established by both the US EPA and the European Union for drinking water. Presumably, if ~0.2–0.3 wt% of PFAS compounds leach into groundwater, they are not suitable for using in land applications.

Table 2 illustrates classifications, groups, and some of the physical/chemical properties of the PFAS detected in the biosolid samples. Analyzing the characteristics of PFAS is beneficial to predict their expected behavior and fate in the environment. The published data on properties of PFAS are very scarce and some are developed by mathematical model rather than by experimentation. The current data reported in Table 2 are extracted from database systems including US EPA toxic chemicals list and PubChem and checked against the literature. The 3D structure of PFAS molecules were drawn using Jmol 14.4.4 software (Table 2).

Table 1. Measured PFAS in biosolids, biochar, biooil, and pyrolysis gas after pyrolysis at 500 and 700 °C.

PFAS (ppb)	S1	500 °C		700 °C		S2	500 °C		700 °C		S3	Test at 500 °C		Test at 700 °C		
	Biosolid	Char	Char	Biosolid	Char	Char	Biosolid	Char	Char	Biosolid	Char	Gas	Oil	Char	Gas	Oil
8:2 Fluorotelomer sulfonic acid (8:2 FTS)	BDL	BDL	BDL	BDL	BDL	BDL	BDL	BDL	BDL	BDL	BDL	BDL	BDL	BDL	BDL	BDL
6:2 Fluorotelomer sulfonic acid (6:2 FTS)	BDL	BDL	BDL	BDL	BDL	BDL	BDL	BDL	BDL	BDL	BDL	BDL	BDL	BDL	BDL	BDL
4:2 Fluorotelomer sulfonic acid (4:2 FTS)	BDL	BDL	BDL	BDL	BDL	BDL	BDL	BDL	BDL	BDL	BDL	BDL	BDL	BDL	BDL	BDL
10:2 Fluorotelomer sulfonic acid (10:2 F)	1.5	BDL	BDL	1.2	BDL	BDL	1.2	BDL	BDL	1.2	BDL	BDL	BDL	BDL	BDL	BDL
Perfluorobutane sulfonic acid (PFBS)	BDL	BDL	BDL	BDL	BDL	BDL	BDL	BDL	BDL	BDL	BDL	BDL	BDL	BDL	BDL	BDL
Perfluorohexane sulfonic acid (PFHxS)	3.8	BDL	BDL	3.6	BDL	BDL	BDL	BDL	BDL	0.45	BDL	BDL	BDL	BDL	BDL	BDL
Perfluorotridecanoic acid (PFTrDA)	BDL	BDL	BDL	BDL	BDL	BDL	BDL	BDL	BDL	BDL	BDL	BDL	BDL	BDL	BDL	BDL
Perfluorooctane sulfonic acid (PFOS)	13.7	BDL	BDL	16.6	BDL	BDL	26.6	BDL	BDL	BDL	BDL	BDL	BDL	BDL	BDL	BDL
Perfluoropentane sulfonic acid (PFPeS)	BDL	BDL	BDL	BDL	BDL	BDL	BDL	BDL	BDL	BDL	BDL	BDL	BDL	BDL	BDL	BDL
N-Et PFO sulfonamide (EtFOSA)	BDL	BDL	BDL	BDL	BDL	BDL	BDL	BDL	BDL	BDL	BDL	BDL	BDL	BDL	BDL	BDL
N-Et PFO sulfonamidoethanol (EtFOSE)	6.3	BDL	BDL	4.8	BDL	BDL	BDL	BDL	BDL	BDL	BDL	BDL	BDL	BDL	BDL	BDL
N-Et PFO sulfonamidoacetic acid (EtFOSAA)	2.9	BDL	BDL	3.2	BDL	BDL	5.3	BDL	BDL	BDL	BDL	BDL	BDL	BDL	BDL	BDL
N-Me PFO sulfonamide (MeFOSA)	BDL	BDL	BDL	BDL	BDL	BDL	BDL	BDL	BDL	BDL	BDL	BDL	BDL	BDL	BDL	BDL
N-Me PFO sulfonamidoacetic acid (MeFOSAA)	3.5	BDL	BDL	2.5	BDL	BDL	2.9	BDL	BDL	BDL	BDL	BDL	BDL	BDL	BDL	BDL
N-Me PFO sulfonamidoethanol (MeFOSE)	BDL	BDL	BDL	BDL	BDL	BDL	BDL	BDL	BDL	BDL	BDL	BDL	BDL	BDL	BDL	BDL
Perfluoroheptane sulfonic acid (PFHpS)	BDL	BDL	BDL	BDL	BDL	BDL	BDL	BDL	BDL	BDL	BDL	BDL	BDL	BDL	BDL	BDL
Perfluorooctane sulfonamide (FOSA)	BDL	BDL	BDL	BDL	BDL	BDL	BDL	BDL	BDL	BDL	BDL	BDL	BDL	BDL	BDL	BDL
Perfluorodecane sulfonic acid (PFDS)	BDL	BDL	BDL	BDL	BDL	BDL	BDL	BDL	BDL	BDL	BDL	BDL	BDL	BDL	BDL	BDL
Perfluorobutanoic acid (PFBA)	BDL	BDL	BDL	BDL	BDL	BDL	BDL	BDL	BDL	N/A	BDL	BDL	N/A	BDL	BDL	BDL
Perfluorodecanoic acid (PFDA)	BDL	BDL	BDL	BDL	BDL	BDL	BDL	BDL	BDL	BDL	BDL	BDL	BDL	BDL	0.04	BDL
Perfluorododecanoic acid (PFDoDA)	BDL	BDL	BDL	BDL	BDL	BDL	BDL	BDL	BDL	BDL	BDL	BDL	BDL	BDL	BDL	BDL
Perfluoroheptanoic acid (PFHpA)	BDL	BDL	BDL	BDL	BDL	BDL	BDL	BDL	BDL	BDL	BDL	BDL	BDL	BDL	BDL	BDL
Perfluorohexanoic acid (PFHxA)	1.6	BDL	BDL	1.8	0.26	0.15	2.2	0.39	19.49	BDL	BDL	BDL	1.44	BDL	BDL	BDL
Perfluorononanoic acid (PFNA)	1.1	BDL	BDL	BDL	BDL	BDL	BDL	BDL	1.68	BDL	BDL	BDL	1.21	BDL	BDL	BDL
Perfluorooctanoic acid (PFOA)	BDL	BDL	BDL	BDL	0.18	BDL	BDL	0.23	2.45	BDL	BDL	BDL	0.61	BDL	BDL	BDL
Perfluoropentanoic acid (PFPeA)	BDL	BDL	BDL	BDL	BDL	BDL	BDL	BDL	4.94	BDL	BDL	BDL	1.04	BDL	BDL	BDL
Perfluorotetradecanoic acid (PFTeDA)	BDL	BDL	BDL	BDL	BDL	BDL	BDL	BDL	BDL	BDL	BDL	BDL	BDL	BDL	BDL	BDL
Perfluoroundecanoic acid (PFUnDA)	1.9	BDL	BDL	BDL	BDL	BDL	BDL	1.8	BDL	0.47	BDL	BDL	0.28	BDL	BDL	BDL
Perfluorononane sulfonic acid (PFNS)	N/A	N/A	N/A	N/A	N/A	N/A	N/A	N/A	N/A	BDL	N/A	N/A	N/A	BDL	N/A	N/A

Table 2. Characteristics of detected PFASs.

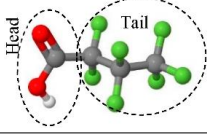
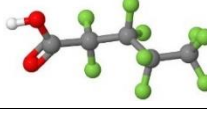
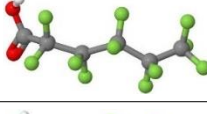
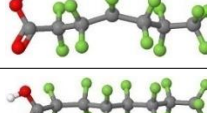
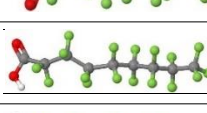
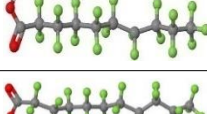
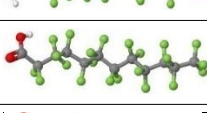
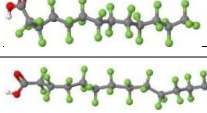
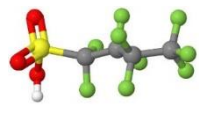
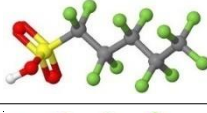
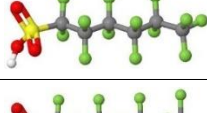
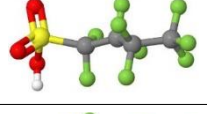
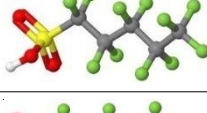
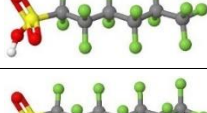
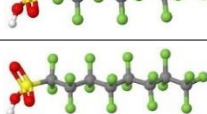
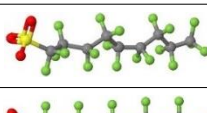
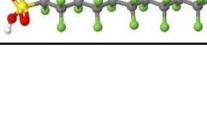

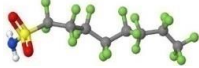
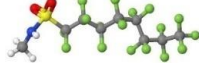
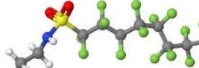



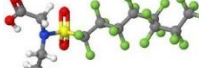

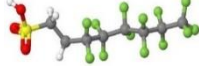
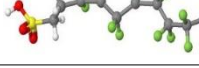
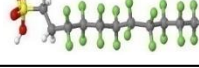
Class	Group	PFAS Acronym	Molecular Formula	Molecular Weight (g/mol)	Chain Length	Molecular Structure	Density (g/cm ³)	Melting Point T _m (°C)	Boiling Point T _b (°C)	Water Solubility (g/L)	Vapor Pressure (Pa)		
Perfluoroalkyl acids (PFAAs)	PFCA (Perfluoroalkyl carboxylic acids)	PFBA	C ₄ HF ₇ O ₂	214.04	SC *		1.61	−17.5	121	N/A	1307		
		PFPeA	C ₅ HF ₉ O ₂	264.05	SC		1.67	N/A	124.4	112.6	1057		
		PFHxA	C ₆ HF ₁₁ O ₂	314.05	SC		1.69	14	143	21.7	457		
		PFHpA	C ₇ HF ₁₃ O ₂	364.06	SC		1.71	30	175	4.2	158		
		PFOA	C ₈ HF ₁₅ O ₂	414.07	LC **		1.80	37–60	188–192	3.4–9.5	4–1300		
		PFNA	C ₉ HF ₁₇ O ₂	464.08	LC		1.78	56–59	218	9.5	1.3		
		PFDA	C ₁₀ HF ₁₉ O ₂	514.09	LC		1.79	77–88	218	9.5	0.2		
		PFUnDA	C ₁₁ HF ₂₁ O ₂	564.09	LC		1.81	83–101	160–230	0.004	0.1		
		PFDoDA	C ₁₂ HF ₂₃ O ₂	614.10	LC		1.82	107–109	245	0.0007	0.01		
		PFTTrDA	C ₁₃ HF ₂₅ O ₂	664.11	LC		1.85	N/A	N/A	0.0002	0.3		
		PFTeDA	C ₁₄ HF ₂₇ O ₂	714.12	LC		1.86	N/A	276	0.00003	0.1		
		PFASs (Perfluoroalkane sulfonic acids)		PFBS	C ₄ HF ₉ SO ₃	300.09	SC		1.81	76–84	211	46.2–56.6	631
				PFPeS	C ₅ HF ₁₁ SO ₃	350.11	SC		N/A	N/A	225	N/A	N/A
				PFHxS	C ₆ HF ₁₃ SO ₃	400.11	LC		N/A	86	226	2.3	58.9
PFHpS	C ₇ HF ₁₅ SO ₃			450.12	LC		N/A	N/A	N/A	N/A	N/A		
PFOS	C ₈ HF ₁₇ SO ₃			500.13	LC		1.84	N/A	>400	1.52–1.57	6.7		
PFNS	C ₉ HF ₁₉ SO ₃			549.13	LC		1.84	183	N/A	N/A	N/A		
PFDS	C ₁₀ HF ₂₁ SO ₃			600.14	LC		N/A	N/A	N/A	0.002	0.71		

Table 2. Cont.

Class	Group	PFAS Acronym	Molecular Formula	Molecular Weight (g/mol)	Chain Length	Molecular Structure	Density (g/cm ³)	Melting Point T _m (°C)	Boiling Point T _b (°C)	Water Solubility (g/L)	Vapor Pressure (Pa)	
Perfluoroalkane Sulfonamides (FASAs)	FASAs	FOSA	C ₈ H ₂ F ₁₇ NSO ₂	499.14	LC		1.79	154–155	N/A	N/A	N/A	
Perfluoroalkane sulfonamido substances	N-alkyl Perfluoroalkane sulfonamides (N-alkyl FASAs)	MeFOSA	C ₉ H ₄ F ₁₇ NSO ₂	513.17	LC		N/A	N/A	N/A	0.0002	0.3	
		EtFOSA	C ₁₀ H ₆ F ₁₇ NSO ₂	527.2	LC		N/A	N/A	N/A	0.0001	0.12	
	Nalkyl perfluoroalkane sulfonamido ethanols (N-alkyl FASEs)	MeFOSE	C ₁₁ H ₈ F ₁₇ NSO ₃	557.22	LC		N/A	N/A	N/A	0.0003	0.0004	
		EtFOSE	C ₁₂ H ₁₀ F ₁₇ NSO ₃	571.25	LC		N/A	55–60	N/A	0.0001	0.002	
	N-alkyl perfluoroalkane sulfonamido acetic acids (N-alkyl FASAAAs)	MeFOSAA	C ₁₁ H ₆ F ₁₇ NSO ₄	571.21	LC		N/A	N/A	N/A	N/A	N/A	
		EtFOSAA	C ₁₂ H ₈ F ₁₇ NSO ₄	585.24	LC		N/A	N/A	N/A	N/A	N/A	
	Fluorotelomer substances	n:2 Fluorotelomer sulfonic acids (n:2 FTSAs)	4:2 FTS	C ₆ H ₅ F ₉ SO ₃	328.15	LC		1.68	N/A	216	27.9	0.33
			6:2 FTS	C ₈ H ₅ F ₁₃ SO ₃	428.16	LC		1.68	69.2	238	1.3	0.11
8:2 FTS			C ₁₀ H ₅ F ₁₇ SO ₃	528.18	LC		1.71	83.8	250	0.06	0.01	
10:2 FTS			C ₁₂ H ₅ F ₂₁ SO ₃	628.2	LC		1.75	173	N/A	0.002	0.001	

* Short Chain, ** Long Chain.

All short-chain types of PFAS were not measurable in all three biosolid samples, excluding PFHxA, which was detected between 1–2.2 ppb in all samples. Shorter-chain PFAS tend to be more soluble in water compared to long ones, showing that these biosolids are not highly susceptible to dissolve such chemicals in ground/surface water if released into the environment as they are mostly contaminated with long-chain PFAS. This can be attributed to a longer hydrophobic carbon–fluorine ‘tail’ in PFAS (Table 2) [29]. Short-chain PFAS are

very mobile and can travel over long distances due to their higher solubility and lower density, in contrast to longer-chain PFAS [30]. As such, the biosolid samples investigated in this work potentially are less able to widely spread in the environment. Sepulvado et al. confirmed a higher transport potential for short-chain PFAS in soils amended with municipal biosolids [31]. Other studies investigated the accumulation of PFAS in agricultural plants and found the longer-chained PFAS are mostly taken up by the roots, while build-up of shorter-chained PFAS occurs more in the leaves/fruits/heads [32,33]. Melting point and boiling point determine the physical state (solid, liquid, and gas) of pure PFAS compounds at environmental temperatures. Higher number of carbon atoms in PFAS chain results in elevation of certain physical properties, such as melting/boiling point [34]. For instance, PFBA is in liquid form at ambient temperature and atmospheric pressure, while PFHxS is a white crystalline powder. Vapor pressure indicates the volatility and tendency of the molecules to evaporate as well as the fate of environmental pollutants in an ecosystem [35]. On the contrary to the melting/boiling points, the vapor pressure of PFAS decreases by increasing fluorinated carbon chain length [36] and, hence, shorter-chain PFAS found in biosolids, such as PFHxA, are capable of broad dispersion after entering the environment.

Impact of Pyrolysis on PFAS Destruction

After pyrolysis performed at 500 °C, PFAS compounds were completely removed from the biochar in the S1 sample and destroyed up to 98.7 wt% in the S2 and 97.3 wt% in the S3 biochars. Thoma et al. [37] also concluded that a low-temperature pyrolysis process could remove >90% of PFOS and PFOA from biosolid-derived biochar. Further reduction was achieved by pyrolyzing the biosolids at 700 °C, with PFAS undetected in the S1 and S3 biochars and reduced by 99.6 wt% in the S2 biochar. The amount of PFAS in the gas- and liquid-phase outputs were also measured for the pyrolysis of the S3 biosolids in order to gain better insight into the fate of PFAS in all product streams. At both pyrolysis temperatures, all detectable PFAS was eliminated from the biooil fraction of sample S3. However, the pyrogas still contained 72.9 wt% of total PFAS present in the S3 original biosolid after the lower pyrolysis temperature of 500 °C. The higher temperature of 700 °C had the noticeable ability to both volatilize and destroy the PFAS compounds (~88 wt%). Most of the remaining PFAS after pyrolysis existed in the gas phase; that is, ~96 and 100 wt% of the remaining PFAS was segregated in the pyrogas after the pyrolysis at 500 and 700 °C, respectively. Of the PFAS constituents which are measurable in the biosolids, 10:2 FTS, PFOS, EtFOSAA, and MeFOSAA were all desorbed from the solid phase of the S3 sample at both test temperatures, and additionally were not present in the pyrogas or biooil, indicating both volatilization and decomposition.

Figure 2 represents each PFAS component in the biosolids, biochar, and pyrogas in terms of their percentage contribution. As previously mentioned, there is no PFAS present in the S1 biochar produced at both temperatures, in the S3 biochar generated at 700 °C, or in the S3 biooil produced at both temperatures, as the components tested were all below the detection limit. In Figure 2, short-chain PFAS are characterized by a black dotted bar, while colorful columns illustrate the long-chain ones. After pyrolysis, most of the long-chain PFAS were distinctly converted to short chains. Approximately 85 wt% of the PFAS in the S2 biosolids and 95 wt% of the PFAS in the S3 biosolids were composed of long-chain PFAS, which were reduced to less than half in all product streams, particularly at the higher pyrolysis temperature (Figure 2). In general, short-chain PFAS persisted more in the biochar as opposed to the pyrogas. This could be attributed to reactions of shorter-chain PFAS in the gas phase and generation of new PFASs with longer chain lengths, such as PFNA and PFDA in the S3 pyrogas produced at 700 °C. On the other hand, fluorotelomer substances, such as 10:2 FTS, possibly oxidize to generate PFCA by reaction with OH radicals [38]. From the environmental point of view, the presence of longer-chain PFAS in gaseous products is less concerning, because they are less mobile and less soluble in water, as described earlier in Section 3.1. Other treatments can be used to further decompose the gaseous PFAS compounds, including recycling gas fraction as a fuel in the pyrolysis

process [34], elevated temperature upgrading [35], and scrubbing and thermal oxidation at high temperatures [36], in which off-gas streams typically break down into water, carbon dioxide, nitrogen, and sulfur dioxide compounds. Thermal oxidizers have been applied in a commercial-scale facility in the US (Silicon Valley Clean Water, California) for combustion of raw off-gas from pyrolysis-inhibiting tar formation [39].

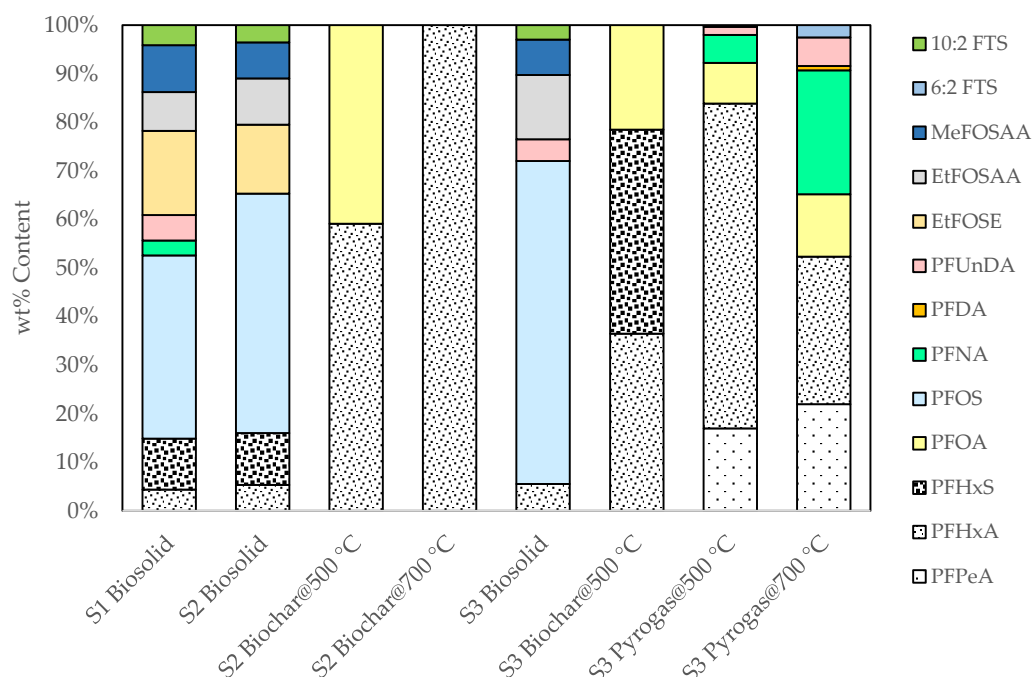


Figure 2. PFAS components (wt%) detected in biosolid, biochar, and pyrogas at 500 and 700 °C. Molecular structure color codes: Carbon: gray; Nitrogen: blue; Hydrogen: white; Oxygen: red; Fluorine: green; Sulfur: yellow.

Overall, it is evident that less harmful products were generated after the pyrolysis process (Figure 2). For instance, PFOS, one of the most stable chemicals [40], was totally eliminated from all samples of biosolids at both pyrolysis temperatures. The high melting/boiling point and two strong bonds of the sulfonic acid functional group (S=O) make PFOS substances more thermally stable and extremely persistent in the environment compared to the PFOA and other PFAS types (Table 2) [41].

It is noteworthy to mention that, in some cases, the concentration appears to increase from below detection limit in the original biosolids to a detectable level in the outputs (Table 1 and Figure 2). For instance, Perfluorooctanoic acid (PFOA) concentration in biochar produced from the S2 sample increased from nondetectable to 0.18 ppb after pyrolysis at 500 °C. This can be attributed to either (1) the overall mass balance, as the concentration of specific type of PFAS, e.g., PFOA, was not high enough to be detected until the mass reduction in converting biosolids to products, or (2) PFAS precursor (such as sulfonamido substances) degradation during pyrolysis, indicating that some compounds may be the result of partial transformation/destruction of other PFAS components [42].

Biochar produced after PFAS elimination from biosolids via pyrolysis is considered ‘Class A Exceptional Quality’, having met all pathogen and vector-attraction reduction requirements, as well as meeting the concentration limits of heavy metals according to the U.S. Environmental Protection Agency’s (EPA) 40 Code of Federal Regulations (CFR) Part 503.32(a) rule [43]. As such, when this biochar is applied to the soil, it can be considered as a valuable fertilizer supplement and soil amendment, an effective agricultural nutrition source, in addition to an effective technique for carbon sequestration.

3.2. Material Balances

The pyrolysis pilot unit operates on a ‘once-through’ basis, and the products are biochar, biooil, and pyrogas. By varying the operating temperatures, the yields of each product stream also vary. For each pyrolysis test, 500 g of feedstock was processed. At 500 °C, this led to output yields of approximately 40 wt% biochar, 40 wt% biooil, and 20 wt% pyrogas. As the temperature increases, the reaction favors the formation of pyrogas, as expected, with the yields at 700 °C being approximately 30 wt% biochar, 33 wt% biooil, and 37 wt% pyrogas. At higher temperatures, more of the volatile species in the solid feedstock are volatilized. In addition, the longer-chain hydrocarbons that are volatilized from the biosolids at 500 °C condense as biooil and are further cracked into gaseous products in the runs at 700 °C.

One of the principal objectives of this study was to determine the fate of the various PFAS components during the pyrolysis of biosolids. For the S3 sample, PFHxS was below detection limits in the biosolids. However, it was measured in the biochar produced at 500 °C (Table 1). Its presence in the biochar is most likely due to a concentrating effect, as the overall solid mass decreases based on the overall mass balance. At 700 °C, no PFHxS was present in any of the streams, and therefore, volatilization and decomposition can be postulated to have occurred. Other components, such as 6:2 FTS, PFDA, PFNA, PFOA, and PFPeA, were also found below detection limit in the biosolids, but were detectable in the pyrolysis products, as discussed earlier. There was no PFOA remaining in the S3 biochar produced at 700 °C, indicating that thermal volatilization had occurred, while there is a reduction in the pyrogas with respect to the 500 °C run, showing that its thermal decomposition occurs between 500 and 700 °C.

3.3. Solids Ash and Energy Analysis

Energy value, elemental analysis, proximate analysis (Table 3), and ash analysis (Table 4) were conducted on the biosolids feedstock and on the biochars produced at 500 and 700 °C. These parameters are beneficial for the design of full-scale pyrolysis systems, and for determining the best market opportunity for the resultant biochars. The higher heating value (HHV) of the biosolids, presented in Table 3, is relatively high at 18.5 MJ/kg, similar to typical woody materials. As the S3 material was pyrolyzed, the HHV decreased to 11.6 and 10.3 for the 500 and 700 °C runs, respectively. This trend has been verified by another study [44] for the rest of the samples. There are two factors contributing to the decrease in HHV:

- (a) Yield and ash concentration. As the total amount of solid product decreases during pyrolysis, the inert ash concentrates in the solid biochar. While the total mass of ash did not change, its concentration increased from 17.9 wt% in the S3 biosolids to 61.4 wt% in the biochar produced at 500 °C, and to 69.7 wt% in the biochar produced at 700 °C. From an energy point of view, ash is an inert constituent and, hence, drastically increasing its concentration will decrease the heating value [45].
- (b) Volatile matter reduction. As the pyrolysis reactor temperature increased, the volatile compounds are vaporized, resulting in less energy-rich volatile matter in the biochar, which, in turn, decreases that contribution toward its calorific value. This devolatilization is consistent with what is typically expected in pyrolysis processes [46]. The decrease in volatile matter in the solid fraction is a benefit from an overall pyrolysis system perspective, as the volatile matter is transferred to the pyrogas stream, based on the overall mass balance. Therefore, as the temperature increases, the energy balance increasingly favors the pyrogas stream, allowing for sufficient energy becoming available to allow the system to not only operate autothermally, exclusively from the energy produced by the pyrogas it generates, but also the opportunity for excess pyrogas being available for other energy uses.

Table 3. Energy, ultimate (dry basis), and proximate analysis (as received).

Parameter	S1 Biosolid	S1 Biochar 500 °C	S1 Biochar 700 °C	S2 Biosolid	S2 Biochar 500 °C	S2 Biochar 700 °C	S3 Biosolid	S3 Biochar 500 °C	S3 Biochar 700 °C	Other work Biosolid [44]	Other work Biochar 500 °C [44]	Other work Biochar 700 °C [44]
HHV (MJ/kg)	10.4	7.8	6.3	15.1	10.5	8.1	18.5	11.6	10.3	14.68	9.9	9.2
Carbon (wt%)	24.02	18.2	15.02	33.03	25.75	22.6	39.95	26.69	23.95	36.71	29.3	26.5
Nitrogen (wt%)	1.29	0.62	0.53	2.83	0.55	0.53	5.87	0.15	0.08	5.42	3.6	3.3
Hydrogen (wt%)	3.93	1.26	0.38	5.08	1.05	0.4	5.83	1.63	0.56	4.24	1.33	1.03
Sulfur (wt%)	0.94	1.24	1.6	1.28	0.92	1	0.54	0.54	0.86	0.92	0.24	0.52
Oxygen (wt%)	25.22	4.28	2.17	27.78	8.23	6.97	29.94	9.57	4.89	23.70	11.47	8.35
Moisture (wt%)	8.9	0.8	0.3	5.3	0.7	0.5	4.48	0.12	2.12	55.7	17.74	12.11
Volatile Matter (wt%)	40.9	11.4	1.3	53.6	14.4	7.2	65.01	10.8	1.66	28.43	54.08	60.3
Ash (wt%)	44.6	74.4	80.3	30	63.5	68.5	17.88	61.43	69.66			

Table 4. Ash analysis.

Parameter (mg/kg)	S1 Biosolid	S1 Biochar 500 °C	S1 Biochar 700 °C	S2 Biosolid	S2 Biochar 500 °C	S2 Biochar 700 °C	S3 Biosolids	Test at 500 °C		Test at 700 °C		EPA Limits * (mg/kg)
								Biochar	Biooil	Biochar	Biooil	
Arsenic	6.00	6.51	9.89	5.22	2.41	4.35	4	BDL	6.18	BDL	7.81	41
Cadmium	2.4	4.0	2.0	2.0	4.1	0.8	2.2	4.0	0.419	3.2	0.079	39
Chromium	59.2	94.9	102	44.0	81.4	74.6	51.6	82.1	2.47	69.00	0.36	-
Cobalt	5.55	8.58	9.54	3.94	5.31	8.14	3.62	6.10	BDL	6.96	BDL	-
Copper	453	733	816	425	883	850	493	853	18.8	886	2.5	1500
Lead	81.1	130	145	74.5	163	136	77.1	137	2.78	146	0.47	300
Mercury	0.61	<0.15	<0.15	0.75	<0.15	<0.15	0.88	0.19	0.634	BDL	0.330	17
Molybdenum	8.09	13.1	14.2	10.8	29.4	18.7	14.6	24.2	0.558	23.3	0.113	-
Nickel	21.2	34.3	44.5	18.0	37.5	43.8	24.1	40.8	2.16	43.9	0.51	420
Potassium	1330	2080	3480	1580	3650	4080	N/A	N/A	N/A	N/A	N/A	-
Phosphorus	N/A	N/A	N/A	42	44	55.5	N/A	N/A	N/A	N/A	N/A	-
Selenium	<1	<1	<1	<1	<1	<1	1	BDL	5.53	BDL	4.13	100
Zinc	862	1270	1390	791	1490	1410	872	1430	37.7	1510	7.4	2800

* Pollutant limits from EPA for Exceptional Quality Standards for biosolids.

As shown in Table 3, the elemental carbon mass fraction decreases with increasing pyrolysis temperature for the biochars of all biosolids, which is in agreement with the literature [44]. Conversely, for lignocellulosic materials, such as wood, the carbon content of biochar increases with increasing pyrolysis temperature [47]. In addition, elemental nitrogen, hydrogen, and oxygen decrease with increasing pyrolysis temperature since pyrolysis is a well-known process to release low-energy molecules (rich in hydrogen and oxygen) from the reacting biomass [48]. The Van Krevelen diagram (Figure 3) illustrates the evolution of the biosolid components during pyrolysis. The molar H/C and O/C ratio uniformly decreased with increasing pyrolysis temperature for all three types of biomasses, suggesting that demethylation (removal of CH₃) and decarboxylation (removal of CO₂) reactions are favored at higher temperatures [49]. The target values of O/C_{org} < 0.4 and H/C_{org} < 0.7 are accepted by both the European Biochar Certificate (EBC) and the International Biochar Initiative (IBI) as carbon stability indicators [50]. Therefore, the biochars produced in this study can be classified as 'stable biochars', which possess a minimum 1000-year half-life when applied to the soil, demonstrating their effectiveness in reducing greenhouse gas emissions and contributing to carbon sequestration and generation of marketable carbon offsets [51].

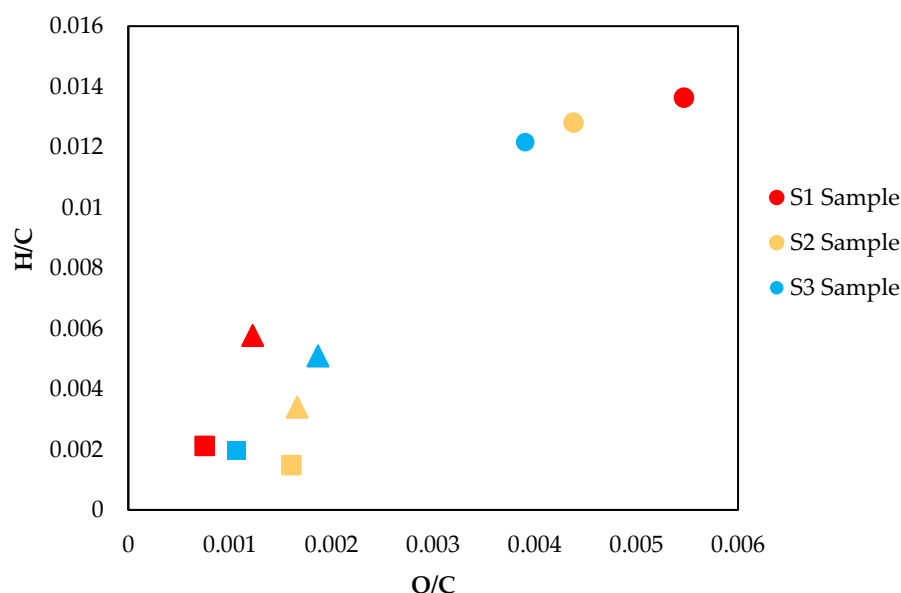


Figure 3. Van Krevelen diagram for biosolids (●) and biochars at 500 °C (▲) and 700 °C (■).

In Table 4, the concentration of the specific ash components (expressed in mg per kg of sample) increased as the ash concentrated in the biochar. Some ash, however, carried through into the condensate (biooil). Of note, both arsenic and selenium were eliminated to below detection limits in the S3 biochar but are present in its biooil. The ash remaining in the biochar is an important factor in determining its marketability, as some ash components, such as potassium and phosphorus detected in some products, are seen to have a positive impact on its quality due to their beneficial properties as fertilizer supplements. On the other hand, other ash components are seen as a negatively affecting its marketability. Therefore, it is important to ensure that they are below local, regional, and federal regulatory or other limits. As an example of one set of regulatory limits, the ash components that could be of concern were compared to the EPA limits for 'Exceptional Quality Standards' for biosolids listed in Table 4. All elements measured in all samples produced were below EPA limits.

4. Conclusions

The overall purpose of this study was to evaluate the ability of high-temperature pyrolysis to eliminate PFAS components present in biosolids. The detectable concentration

of PFAS in the solid biochar product stream is reduced by 97 to 100 wt% at a processing temperature of 500 °C, and by 99.6 to 100 wt% at a processing temperature of 700 °C. Considering all product streams (biochar, biooil, and pyrogas), the measured PFAS is reduced by 88.2 wt% at 700 °C. Therefore, high-temperature pyrolysis (HTP) is demonstrated to be an effective method to drastically reduce the presence of PFAS in biosolids, resulting in extremely low to nondetectable concentrations in the biocarbon output at 700 °C.

Future work will involve the analysis of PFAS evolution in the gas phase at high temperature and in the absence of oxygen during pyrolysis processes at different temperatures. From the preliminary results presented in this work, there are various PFAS components which are below detection limits in the biosolids. However, they are present in the pyrolysis gas at low concentrations. Additional future work on the pyrogas is recommended to broadening the gas testing parameters for other fluorine compounds, such as hydrogen fluoride (HF). As the high-temperature pyrolysis process is oxygen free, many undesirable compounds would not form. However, determining the presence of HF would allow for further optimization of pyrogas treatment processes and materials of construction for full commercial-scale systems. The ultimate goal of a commercial HTP system is to create as many value-added products as possible from diverse wastes, with the added potential for converting pyrogas to renewable natural gas with high energy value.

Author Contributions: Conceptualization, H.B. and S.P.; methodology, H.B.; validation, H.B. and S.P.; formal analysis, E.M.; investigation, S.P.; resources, F.B.; data curation, E.M.; writing—original draft preparation, H.B.; writing—review and editing, S.P., F.B., and E.M.; supervision, F.B. and S.P.; project administration, F.B.; funding acquisition, F.B. All authors have read and agreed to the published version of the manuscript.

Funding: The Natural Sciences and Engineering Research Council of Canada through the Industrial Research Chair Program in "Thermochemical Conversion of Biomass and Waste to BioIndustrial Resources" and of the industry partners, in particular of Char Technologies Ltd.

Informed Consent Statement: Not applicable.

Data Availability Statement: Not applicable.

Conflicts of Interest: The authors declare no conflict of interest.

References

1. Hutchinson, S.; Rieck, T.; Wu, X. Advanced PFAS precursor digestion methods for biosolids. *Environ. Chem.* **2020**, *17*, 558. [[CrossRef](#)]
2. Armstrong, D.L.; Lozano, N.; Rice, C.P.; Ramirez, M.; Torrents, A. Temporal trends of perfluoroalkyl substances in limed biosolids from a large municipal water resource recovery facility. *J. Environ. Manag.* **2016**, *165*, 88–95. [[CrossRef](#)] [[PubMed](#)]
3. Chambers, B.J.; Nicholson, F.A.; Aitken, M.; Cartmell, E.; Rowlands, C. Benefits of biosolids to soil quality and fertility. *Water Environ. J.* **2003**, *17*, 162–167. [[CrossRef](#)]
4. Letcher, R.J.; Chu, S.; Smyth, S.-A. Side-chain fluorinated polymer surfactants in biosolids from wastewater treatment plants. *J. Hazard. Mater.* **2020**, *388*, 122044. [[CrossRef](#)]
5. Ebrahimi, F.; Lewis, A.J.; Sales, C.M.; Suri, R.; McKenzie, E.R. Linking PFAS partitioning behavior in sewage solids to the solid characteristics, solution chemistry, and treatment processes. *Chemosphere* **2021**, *271*, 129530. [[CrossRef](#)]
6. Gallen, C.; Eaglesham, G.; Drage, D.; Nguyen, T.H.; Mueller, J. A mass estimate of perfluoroalkyl substance (PFAS) release from Australian wastewater treatment plants. *Chemosphere* **2018**, *208*, 975–983. [[CrossRef](#)]
7. Venkatesan, A.K.; Halden, R.U. National inventory of perfluoroalkyl substances in archived U.S. biosolids from the 2001 EPA National Sewage Sludge Survey. *J. Hazard. Mater.* **2013**, *252–253*, 413–418. [[CrossRef](#)]
8. Lee, H.; Tevlin, A.G.; Mabury, S.A. Fate of Polyfluoroalkyl Phosphate Diesters and Their Metabolites in Biosolids-Applied Soil: Biodegradation and Plant Uptake in Greenhouse and Field Experiments. *Environ. Sci. Technol.* **2013**, *48*, 340–349. [[CrossRef](#)] [[PubMed](#)]
9. Schulz, K.; Silva, M.R.; Klaper, R. Distribution and effects of branched versus linear isomers of PFOA, PFOS, and PFHxS: A review of recent literature. *Sci. Total Environ.* **2020**, *733*, 139186. [[CrossRef](#)]
10. Buck, R.C.; Franklin, J.; Berger, U.; Conder, J.M.; Cousins, I.T.; De Voogt, P.; Jensen, A.A.; Kannan, K.; Mabury, S.A.; Van Leeuwen, S.P. Perfluoroalkyl and polyfluoroalkyl substances in the environment: Terminology, classification, and origins. *Integr. Environ. Assess. Manag.* **2011**, *7*, 513–541. [[CrossRef](#)] [[PubMed](#)]

11. OECD. *Synthesis Paper on Per- and Polyfluorinated Chemicals (PFCs), Environment, Health and Safety, Environment Direc-Torate*; OECD: Paris, France, 2013.
12. Crone, B.C.; Speth, T.F.; Wahman, D.G.; Smith, S.J.; Abulikemu, G.; Kleiner, E.J.; Pressman, J.G. Occurrence of per- and polyfluoroalkyl substances (PFAS) in source water and their treatment in drinking water. *Crit. Rev. Environ. Sci. Technol.* **2019**, *49*, 2359–2396. [[CrossRef](#)]
13. Rodowa, A.; Christie, E.; Sedlak, J.; Peaslee, G.; Bogdan, D.; DiGuiseppi, B.; Field, J.A. Field Sampling Materials Unlikely Source of Contamination for Perfluoroalkyl and Polyfluoroalkyl Substances in Field Samples. *Environ. Sci. Technol. Lett.* **2020**, *7*, 156–163. [[CrossRef](#)]
14. Goldenman, G.; Fernandes, M.; Holland, M.; Tugran, T.; Nordin, A.; Schoumacher, C.; McNeill, A. *The Cost of Inaction: A Socioeconomic Analysis of Environmental and Health Impacts Linked to Exposure to PFAS*; Nordic Council of Ministers: Copenhagen, Denmark, 2019.
15. Garg, S.; Wang, J.; Kumar, P.; Mishra, V.; Arafat, H.; Sharma, R.S.; Dumée, L.F. Remediation of water from per-/poly-fluoroalkyl substances (PFAS)—Challenges and perspectives. *J. Environ. Chem. Eng.* **2021**, *9*, 105784. [[CrossRef](#)]
16. Liu, C.J.; McKay, G.; Jiang, D.; Tenorio, R.; Cath, J.T.; Amador, C.; Murray, C.C.; Brown, J.B.; Wright, H.B.; Schaefer, C.; et al. Pilot-scale field demonstration of a hybrid nanofiltration and UV-sulfite treatment train for groundwater contaminated by per- and polyfluoroalkyl substances (PFASs). *Water Res.* **2021**, *205*, 117677. [[CrossRef](#)] [[PubMed](#)]
17. Enschede, M.; Rusinek, C.A.; Becker, M.F.; Schuelke, T. A combined current density technique for the electrochemical oxidation of perfluorooctanoic acid (PFOA) with boron-doped diamond. *Water Environ. J.* **2020**, *35*, 158–165. [[CrossRef](#)]
18. Berg, C.; Crone, B.; Gullett, B.; Higuchi, M.; Krause, M.J.; Lemieux, P.M.; Martin, T.; Shields, E.P.; Struble, E.; Thoma, E.; et al. Developing innovative treatment technologies for PFAS-containing wastes. *J. Air Waste Manag. Assoc.* **2022**, *72*, 540–555. [[CrossRef](#)]
19. Tran, T.; Abrell, L.; Brusseau, M.L.; Chorover, J. Iron-activated persulfate oxidation degrades aqueous Perfluorooctanoic acid (PFOA) at ambient temperature. *Chemosphere* **2021**, *281*, 130824. [[CrossRef](#)]
20. Cao, H.; Zhang, W.; Wang, C.; Liang, Y. Sonochemical degradation of poly- and perfluoroalkyl substances—A review. *Ultrason. Sonochem.* **2020**, *69*, 105245. [[CrossRef](#)]
21. Wanninayake, D.M. Comparison of currently available PFAS remediation technologies in water: A review. *J. Environ. Manag.* **2021**, *283*, 111977. [[CrossRef](#)]
22. Mohamed, B.A.; Li, L.Y.; Hamid, H.; Jeronimo, M. Sludge-based activated carbon and its application in the removal of perfluoroalkyl substances: A feasible approach towards a circular economy. *Chemosphere* **2022**, *294*, 133707. [[CrossRef](#)]
23. ITRC. *Remediation Technologies and Methods for Per- and Polyfluoroalkyl Substances (PFAS)*; Interstate Technology Regu Count Sheets: Arlington, TX, USA, 2018.
24. Winchell, L.J.; Ross, J.J.; Wells, M.J.M.; Fonoll, X.; Norton, J.W., Jr.; Bell, K.Y. Per- and polyfluoroalkyl substances thermal destruction at water resource recovery facilities: A state of the science review. *Water Environ. Res.* **2020**, *93*, 826–843. [[CrossRef](#)]
25. Longendyke, G.K.; Katel, S.; Wang, Y. PFAS fate and destruction mechanisms during thermal treatment: A comprehensive review. *Environ. Sci. Process. Impacts* **2021**, *24*, 196–208. [[CrossRef](#)] [[PubMed](#)]
26. Bolan, N.; Sarkar, B.; Yan, Y.; Li, Q.; Wijesekara, H.; Kannan, K.; Tsang, D.C.; Schauerte, M.; Bosch, J.; Noll, H.; et al. Remediation of poly- and perfluoroalkyl substances (PFAS) contaminated soils—To mobilize or to immobilize or to degrade? *J. Hazard. Mater.* **2020**, *401*, 123892. [[CrossRef](#)] [[PubMed](#)]
27. Sharma, R.; Sharma, M.; Sharma, R.; Sharma, V. The impact of incinerators on human health and environment. *Rev. Environ. Heal.* **2013**, *28*, 67–72. [[CrossRef](#)]
28. Liu, C.J.; Werner, D.; Bellona, C. Removal of per- and polyfluoroalkyl substances (PFASs) from contaminated groundwater using granular activated carbon: A pilot-scale study with breakthrough modeling. *Environ. Sci. Water Res. Technol.* **2019**, *5*, 1844–1853. [[CrossRef](#)]
29. Fernandez, N.A.; Rodriguez-Freire, L.; Keswani, M.; Sierra-Alvarez, R. Effect of chemical structure on the sonochemical degradation of perfluoroalkyl and polyfluoroalkyl substances (PFASs). *Environ. Sci. Water Res. Technol.* **2016**, *2*, 975–983. [[CrossRef](#)]
30. Brendel, S.; Fetter, E.; Staude, C.; Vierke, L.; Biegel-Engler, A. Short-chain perfluoroalkyl acids: Environmental concerns and a regulatory strategy under REACH. *Environ. Sci. Eur.* **2018**, *30*, 9. [[CrossRef](#)]
31. Sepulvado, J.G.; Blaine, A.C.; Hundal, L.S.; Higgins, C.P. Occurrence and Fate of Perfluorochemicals in Soil Following the Land Application of Municipal Biosolids. *Environ. Sci. Technol.* **2011**, *45*, 8106–8112. [[CrossRef](#)]
32. Navarro, I.; de la Torre, A.; Sanz, P.; Porcel, M.; Pro, J.; Carbonell, G.; Martínez, M.D.L. Uptake of perfluoroalkyl substances and halogenated flame retardants by crop plants grown in biosolids-amended soils. *Environ. Res.* **2017**, *152*, 199–206. [[CrossRef](#)]
33. Ghisi, R.; Vamerli, T.; Manzetti, S. Accumulation of perfluorinated alkyl substances (PFAS) in agricultural plants: A review. *Environ. Res.* **2018**, *169*, 326–341. [[CrossRef](#)]
34. Mahinroosta, R.; Senevirathna, L. A review of the emerging treatment technologies for PFAS contaminated soils. *J. Environ. Manag.* **2019**, *255*, 109896. [[CrossRef](#)] [[PubMed](#)]
35. Bhatarai, B.; Gramatica, P. Correction to Prediction of Aqueous Solubility, Vapor Pressure and Critical Micelle Concentration for Aquatic Partitioning of Perfluorinated Chemicals. *Environ. Sci. Technol.* **2011**, *46*, 566. [[CrossRef](#)]

36. Rahman, M.F.; Peldszus, S.; Anderson, W.B. Behaviour and fate of perfluoroalkyl and polyfluoroalkyl substances (PFASs) in drinking water treatment: A review. *Water Res.* **2014**, *50*, 318–340. [[CrossRef](#)]
37. Thoma, E.D.; Wright, R.S.; George, I.; Krause, M.; Presezzi, D.; Villa, V.; Preston, W.; Deshmukh, P.; Kauppi, P.; Zemek, P.G. Pyrolysis processing of PFAS-impacted biosolids, a pilot study. *J. Air Waste Manag. Assoc.* **2022**, *72*, 309–318. [[CrossRef](#)] [[PubMed](#)]
38. Winchell, L.J.; Wells, M.J.M.; Ross, J.J.; Fonoll, X.; Norton, J.W., Jr.; Kuplicki, S.; Khan, M.; Bell, K.Y. Per- and Polyfluoroalkyl Substances Presence, Pathways, and Cycling through Drinking Water and Wastewater Treatment. *J. Environ. Eng.* **2022**, *148*, 03121003. [[CrossRef](#)]
39. Winchell, L.J.; Ross, J.J.; Brose, D.A.; Pluth, T.B.; Fonoll, X.; Norton, J.W.; Bell, K.Y. Pyrolysis and gasification at water resource recovery facilities: Status of the industry. *Water Environ. Res.* **2022**, *94*, e10701. [[CrossRef](#)]
40. Johansson, N.; Fredriksson, A.; Eriksson, P. Neonatal exposure to perfluorooctane sulfonate (PFOS) and perfluorooctanoic acid (PFOA) causes neurobehavioural defects in adult mice. *NeuroToxicology* **2008**, *29*, 160–169. [[CrossRef](#)]
41. Baran, J.R. Fluorinated Surfactants and Repellents: Second Edition, Revised and Expanded Surfactant Science Series. Volume 97. By Erik Kissa (Consultant, Wilmington, DE). Marcel Dekker: New York. 2001. xiv + 616 pp. \$195.00. ISBN 0-8247-0472-X. *J. Am. Chem. Soc.* **2001**, *123*, 8882. [[CrossRef](#)]
42. OECD. Preliminary Lists of PFOS, PFAS, PFOA and Related Compounds and Chemicals that May Degrade to PFCA. *OECD Pap.* **2006**, *6*, 1–194. [[CrossRef](#)]
43. US Environmental Protection Agency (EPA). *A Plain English Guide to the EPA Part 503 Biosolids Rule Excellence in Compliance Through*; EPA-832/R-93/003; EPA: Washington, DC, USA, 1994.
44. Rathnayake, N.; Patel, S.; Halder, P.; Aktar, S.; Pazferreiro, J.; Sharma, A.; Surapaneni, A.; Shah, K. Co-pyrolysis of biosolids with alum sludge: Effect of temperature and mixing ratio on product properties. *J. Anal. Appl. Pyrolysis* **2022**, *163*, 105488. [[CrossRef](#)]
45. Hytönen, J.; Nurmi, J. *Heating Value and Ash Content of Intensively Managed Stands*; Wood Research: Kannus, Finland, 2015.
46. Kung, K.S.; Thengane, S.K.; Shanbhogue, S.; Ghoniem, A.F. Parametric analysis of torrefaction reactor operating under oxygen-lean conditions. *Energy* **2019**, *181*, 603–614. [[CrossRef](#)]
47. Bamdad, H.; Hawboldt, K.; MacQuarrie, S.; Papari, S. Application of biochar for acid gas removal: Experimental and statistical analysis using CO₂. *Environ. Sci. Pollut. Res.* **2019**, *26*, 10902–10915. [[CrossRef](#)]
48. Bamdad, H.; Hawboldt, K.; MacQuarrie, S. A review on common adsorbents for acid gases removal: Focus on biochar. *Renew. Sustain. Energy Rev.* **2018**, *81*, 1705–1720. [[CrossRef](#)]
49. Kundu, S.; Patel, S.; Halder, P.; Patel, T.; Marzbali, M.H.; Pramanik, B.K.; Paz-Ferreiro, J.; de Figueiredo, C.C.; Bergmann, D.; Surapaneni, A.; et al. Removal of PFASs from biosolids using a semi-pilot scale pyrolysis reactor and the application of biosolids derived biochar for the removal of PFASs from contaminated water. *Environ. Sci. Water Res. Technol.* **2020**, *7*, 638–649. [[CrossRef](#)]
50. Leng, L.; Huang, H.; Li, H.; Li, J.; Zhou, W. Biochar stability assessment methods: A review. *Sci. Total Environ.* **2018**, *647*, 210–222. [[CrossRef](#)]
51. Bamdad, H.; Papari, S.; Lazarovits, G.; Berruti, F. Soil amendments for sustainable agriculture: Microbial organic fertilizers. *Soil Use Manag.* **2021**, *38*, 94–120. [[CrossRef](#)]